

Coherent ρ^0 Photoproduction in Complex Nuclei*

KURT GOTTFRIED†

*Laboratory of Nuclear Science and Physics Department, Massachusetts Institute of Technology,
Cambridge, Massachusetts 02139*

and

Laboratory of Nuclear Studies, Cornell University, Ithaca, New York 14850

AND

DAVID I. JULIUS

Laboratory of Nuclear Studies, Cornell University, Ithaca, New York 14850

(Received 25 August 1969)

The major purpose of this paper is a description of coherent ρ photoproduction which takes the rather substantial width of the ρ into proper account. The optical-model analysis due to Drell and Trefil is extended to include ρ decay inside the nucleus, as well as the subsequent absorption of the decay pions. The eikonal method is used throughout, and is found to yield compact analytic expressions for the production amplitude. The decay effects produce an appreciable shift of the ρ peak towards lower mass for production in heavy nuclei and at the lower photon energies of current interest (2.7–4.5 GeV). On the whole, the differential cross sections are not significantly affected in either shape or magnitude by the effects arising from ρ decay. In particular, the decay corrections do not appreciably influence the determination via vector dominance of the ρ -photon coupling constant.

I. INTRODUCTION

DURING the past two years several laboratories have announced results of elegant experiments on coherent ρ^0 photoproduction from complex nuclei.^{1–7} Measurements have been made of the ρ^0 differential production cross sections from a wide variety of nuclei over a large energy range, and the $\pi\pi$ -mass spectrum has also been determined. These data provide information on the ρ^0 -nucleon total cross section, and the ρ^0 -photon coupling constant.

The data analysis has largely been based on the theory of Drell and Trefil⁸; we shall refer to this work by DT henceforth. In DT the very considerable ρ^0 width is ignored, and the $\pi\pi$ -mass spectrum is tacitly assumed to be the same as in production from a single nucleon. It is our main purpose in this paper to describe

a simple extension of the DT theory that correctly incorporates the possibility of ρ decay inside the nucleus.

The full $\pi\pi$ -production amplitude is a coherent sum of two parts: a term that describes ρ decay outside the nucleus, and another wherein the ρ decays inside the nucleus. The former dominates at high energy ($\gtrsim 5$ GeV) in even the heaviest nuclei. The interior decay amplitude has a $\pi\pi$ -mass spectrum that differs very markedly from that of ρ decay in vacuum because of a process closely akin to ordinary collision broadening. The exterior amplitude has a mass spectrum that differs somewhat from that of vacuum decay because the minimum transfer Q increases with $\pi\pi$ mass, and the decrease of the nuclear form factor with Q therefore skews the mass distribution towards low masses. Aside from these modifications of the mass spectrum, there is also some effect on the magnitude of the differential cross section for ρ production arising from the difference in nuclear mean free path between the ρ and its decay products; that is, the $\pi\pi$ state has greater difficulty in escaping the nucleus than does the ρ itself.

Our detailed calculations shall show that on the whole the DT theory works remarkably well.⁹ The most important correction due to ρ instability is an appreciable shift of the $\pi\pi$ resonance to lower mass in medium weight and heavy nuclei for photon energies below 5 GeV. A similar shift was observed in the earliest experiments on ρ production,^{1,2} and subsequently claimed to be a consequence of vector dominance by Ross and Stodolsky.¹⁰ We shall argue that their explanation of the mass shift cannot be inferred from any of the conventional formulations of vector dominance.

* Work supported in part by the Atomic Energy Commission, under Contract No. AT(30-1)2098 at MIT, and by the Office of Naval Research at Cornell University.

† On leave from Cornell University, Ithaca, N. Y., during the academic year 1968–1969.

¹ L. J. Lanzerotti, R. B. Blumenthal, D. C. Ehn, W. L. Faissler, P. M. Joseph, F. M. Pipkin, J. K. Randolph, J. J. Russell, D. G. Stairs, and J. Tenenbaum, *Phys. Rev. Letters* **15**, 210 (1965).

² Aachen-Berlin-Bonn-Hamburg-Heidelberg-München Collaboration, *Nuovo Cimento* **41A**, 270 (1966).

³ J. G. Asbury, U. Becker, W. K. Bertram, P. Joos, M. Rohde, A. J. S. Smith, C. L. Jordan, and S. C. C. Ting, *Phys. Rev. Letters* **19**, 865 (1967); **20**, 1134(E) (1968).

⁴ J. G. Asbury, U. Becker, W. K. Bertram, M. Binkley, E. Coleman, C. L. Jordan, M. Rohde, A. J. S. Smith, and S. C. C. Ting, *Phys. Rev. Letters* **20**, 227 (1968).

⁵ L. J. Lanzerotti, R. B. Blumenthal, D. C. Ehn, W. L. Faissler, P. M. Joseph, F. M. Pipkin, J. K. Randolph, J. J. Russell, D. G. Stairs, and J. Tenenbaum, *Phys. Rev.* **166**, 1365 (1968).

⁶ G. McClellan, N. Mistry, P. Mostek, H. Ogren, A. Silverman, J. Swartz, and R. Talman, *Phys. Rev. Letters* **22**, 377 (1969).

⁷ F. Bulos, W. Busza, R. Giese, R. R. Larsen, D. W. G. S. Leith, B. Richter, V. Perez-Mendez, A. Stetz, S. H. Williams, M. Beniston, and J. Rettberg, *Phys. Rev. Letters* **22**, 490 (1969).

⁸ S. D. Drell and J. S. Trefil, *Phys. Rev. Letters* **16**, 552 (1966); **16**, 832(E) (1966).

⁹ The essential features of these calculations were first reported in an invited paper presented at the Boston meeting of the American Physical Society, February, 1968 (unpublished); see K. Gottfried, *Bull. Am. Phys. Soc.* **13**, 175 (1968).

¹⁰ M. Ross and L. Stodolsky, *Phys. Rev.* **149**, 1172 (1966).

Insofar as the basic photon- ρ coupling constant γ_ρ is concerned, our work unfortunately sheds no light on the discrepancy between the measurements of that constant as determined from the leptonic branching ratio¹¹ and the DESY ρ -production data³ on the one hand, and the Cornell⁶ and SLAC⁷ data on the other.

II. PHOTOPRODUCTION OF AN UNSTABLE ρ^0

We write the coherent photoproduction amplitude for two pions as

$$\mathcal{F} = 4\pi\gamma_{\rho\pi\pi}f_{\rho N}\hat{\epsilon}\cdot(\mathbf{q}_1 - \mathbf{q}_2)F, \quad (1)$$

where $\gamma_{\rho\pi\pi}$ is the $\rho\pi\pi$ coupling constant, $f_{\rho N}$ is the forward ρ -photoproduction amplitude from a single nucleon, \mathbf{q}_i is the momentum of the i th pion, and $\hat{\epsilon}$ is the photon polarization vector. Vector dominance relates $f_{\rho N}$ to the ρN elastic scattering amplitude, but for now we shall proceed without making this hypothesis. The normalization of $f_{\rho N}$ is such that if the ρ were stable, its photoproduction differential cross section would be $|f_{\rho N}|^2 p/k$, where \mathbf{k} and \mathbf{p} are the photon and ρ momenta. The definition of $\gamma_{\rho\pi\pi}$ is such that the $\rho \rightarrow 2\pi$ decay rate is

$$R_{\rho \rightarrow 2\pi} = \frac{1}{48\pi}\gamma_{\rho\pi\pi}^2 \frac{(m_\rho^2 - 4m_\pi^2)^{3/2}}{m_\rho^2}. \quad (2)$$

The physically measurable double-pion-production cross section is found to be

$$\frac{d\sigma}{d\Omega dm^2} = \frac{1}{\pi k} |f_{\rho N}|^2 |F|^2 m_\rho \Gamma_\rho(m), \quad (3)$$

where m is the $\pi\pi$ invariant mass, $d\Omega$ is the element of solid angle for the two-pion total momentum $\mathbf{p} = \mathbf{q}_1 + \mathbf{q}_2$, and

$$\Gamma_\rho(m) = \frac{1}{48\pi}\gamma_{\rho\pi\pi}^2 \frac{(m^2 - 4m_\pi^2)^{3/2}}{m_\rho m}. \quad (4)$$

Several assumptions not yet stated have been incorporated into the foregoing equations. In (1) we have ignored all dependence of the production amplitude on nucleon spins. This is expected to be a good approximation in complex nuclei where the total spin is invariably small compared to the mass number. Furthermore, the ρ -photoproduction data from hydrogen and deuterium¹² indicate a reasonably small spin de-

pendence of the basic one-nucleon amplitudes. The most controversial and intractable tacit assumption concerns the mass dependence given by Eq. (4). This mass dependence can be derived by at least two approximate arguments: (i) from perturbation theory, by treating the ρ as a quasistable particle,¹³ and (ii) from an effective-range formula for $\pi\pi$ p -wave scattering.¹⁴ Both arguments involve uncontrollable, and related, approximations. In (i) one must neglect any change of the decay vertex as the mass of the final state varies; in (ii) one must ignore the shape-dependent term in the effective-range formula. The ambiguities resulting from these approximations are not of great significance as m varies across the peak of the ρ resonance, and we shall therefore use (4) as it stands in comparing our calculations with the data. Naturally, this implies that refined departures in the ρ shape from that given by (4) are outside the scope of our work, but this is hardly surprising: In all branches of physics the shape of a broad resonance depends on the details of the underlying dynamics, and we do not, in this work, address ourselves to the dynamics of $\pi\pi$ scattering. All that we are concerned with is the influence of the nucleus on the shape of the resonance, and if we stay within about 100 MeV of m_ρ , Eq. (4) suffices for this purpose. In extracting the ρ - γ coupling parameter γ_ρ , however, and comparing the result to the leptonic branching ratio, one must extrapolate in m from $m=0$ to $m=m_\rho$, and then the mass-dependent effects just alluded to could be of considerable significance.¹⁴ But none of the model calculations¹⁴ reported appears to provide enough variation to account for the large discrepancy between the Cornell-SLAC results and the leptonic branching ratio. It goes without saying that the difference in γ_ρ as found by DESY and Cornell-SLAC cannot be ascribed to any shortcomings in Eq. (4).

We now turn to the evaluation of the nuclear production amplitude. At high energy the ρ -production and decay vertices can be treated as if they were local, and F can be written as

$$F = \int d^3r' d^3r \phi_{a_1}^*(\mathbf{r}') \phi_{a_2}^*(\mathbf{r}') \mathcal{G}(\mathbf{r}', \mathbf{r}) n(\mathbf{r}) e^{i\mathbf{k}\cdot\mathbf{r}}. \quad (5)$$

Here \mathbf{r} is the γ - ρ conversion point, \mathbf{r}' is the ρ decay point, $\phi_a(\mathbf{r})$ is a pion wave function of asymptotic momentum \mathbf{q} , $n(\mathbf{r})$ is the nuclear density, and \mathcal{G} is the ρ -meson propagator.

\mathcal{G} describes the off-mass-shell propagation of the unstable ρ whether it is in vacuum or in nuclear matter.

¹³ J. D. Jackson, *Nuovo Cimento* **34**, 1644 (1964).

¹¹ V. L. Auslander, G. I. Budker, Ju. N. Pestov, V. A. Sidorov, A. N. Shrinsky, and A. G. Khabakhpashev, *Phys. Letters* **25B**, 433 (1967); J. E. Augustin, D. Benaksas, J. C. Bizot, J. Buon, B. Delcourt, V. Gracco, J. Haissinski, J. Jeanjean, D. Lalanne, F. Laplanche, J. LeFrancis, P. Lehmann, P. Marin, H. Nguyen Ngoc, J. Perez-y-Jorba, F. Richard, F. Rumpf, E. Silva, S. Tavenier, and D. Trielle, *ibid.* **28B**, 503 (1969); S. C. C. Ting, in *Proceedings of the Fourteenth International Conference on High-Energy Physics, Vienna, 1968* (CERN, Geneva, 1968), p. 43.

¹² G. McClellan, N. Mistry, P. Mostek, H. Ogren, A. Silverman, J. Swartz, R. Talman, K. Gottfried, and A. I. Lebedev, *Phys. Rev. Letters* **22**, 374 (1969).

¹⁴ G. J. Gounaris and J. J. Sakurai, *Phys. Rev. Letters* **21**, 244 (1968). Further examination of the effective-range approach reveals that the leptonic branching ratio is distressingly sensitive to the shape-dependent term in the effective-range formula [K. Gottfried (to be published)]. See also D. A. Geffen and T. Walsh, *Phys. Rev. Letters* **20**, 1536 (1968); **21**, 715(E) (1968); M. T. Vaughn, M. L. Blackmon, and K. C. Wali, in *Proceedings of the Fourteenth International Conference on High-Energy Physics, Vienna, 1968* (CERN, Geneva, 1968).

It satisfies the inhomogeneous wave equation¹⁵

$$[\nabla^2 + k^2 - m_\rho^2 + i\Gamma_\rho m_\rho - U(r)]\mathcal{G}(\mathbf{r}', \mathbf{r}) = \delta(\mathbf{r} - \mathbf{r}'), \quad (6)$$

where $U(r) = -ip\sigma_{\rho N}n(r)$ is the optical potential, which we assume to be purely absorptive at the energies in question. The effects of a possible refractive component to the potential are discussed briefly in Sec. IV.

It is advantageous to convert (6) into an equation for

$$G(\mathbf{r}; \mathbf{p}m) \equiv \int d^3r' \phi_{q_1}^*(\mathbf{r}') \phi_{q_2}^*(\mathbf{r}') \mathcal{G}(\mathbf{r}', \mathbf{r}), \quad (7)$$

i.e.,

$$[\nabla^2 + k^2 - m_\rho^2 + i\Gamma_\rho m_\rho - U(r)]G(\mathbf{r}; \mathbf{p}) = \phi_{q_1}^*(\mathbf{r}) \phi_{q_2}^*(\mathbf{r}), \quad (8)$$

where $\mathbf{p} = \mathbf{q}_1 + \mathbf{q}_2$ can be called the momentum of the ρ meson and $m = (k^2 - p^2)^{1/2}$ is the invariant $\pi\pi$ mass. We treat both G and ϕ with the eikonal approximation. In the case of G , this entails two essential assumptions:

(i) The function

$$Y(b, z; \mathbf{p}m) \equiv e^{i\mathbf{p} \cdot \mathbf{r}} G(\mathbf{r}; \mathbf{p}m) \quad (9)$$

varies slowly with z , the coordinate along \mathbf{k} , and (ii) the production angle θ between \mathbf{p} and \mathbf{k} is small enough to allow the replacement $\theta \rightarrow 0$ in the evaluation of Y . With these approximations, (8) reduces to an ordinary differential equation for each value of the impact parameter b ,

$$[\Delta^{-1}(m) + ip\sigma_{\rho N}n(b, z) - 2ip(\partial/\partial z)] \times Y(b, z) = e^{-\Phi(b, z)}, \quad (10)$$

where $\Delta(m) = (m^2 - m_\rho^2 + i\Gamma_\rho m_\rho)^{-1}$ is the vacuum ρ propagator, and

$$\Phi(b, z) = \sigma_{\pi N} \int_z^\infty dz' n(b, z'). \quad (11)$$

We have neglected the finite opening angle between the pion trajectories in evaluating the pion attenuation factor Φ . The solution of (10) is elementary:

$$Y(b, z) = \frac{1}{2ip} e^{-\Psi(b, z)} \int_z^\infty dz' e^{[\Psi(b, z') - \Phi(b, z')]}, \quad (12)$$

where

$$\Psi(b, z) = \frac{iz}{2p\Delta(m)} + \frac{1}{2}\sigma_{\rho N} \int_z^\infty dz' n(b, z'). \quad (13)$$

It is clear that $G(\mathbf{r}, \mathbf{p})$ is the probability amplitude for finding two pions of total momentum \mathbf{p} if a ρ is produced at \mathbf{r} . A closer examination of (12) also reveals that the integration point (b, z') can be interpreted quite unambiguously as the decay point.

Returning to (5), we find in the usual way that

$$F(\theta, m) = 2\pi \int_0^\infty b db \int_{-\infty}^\infty dz e^{iQz} J_0(pb\theta) Y(b, z) n(b, z), \quad (14)$$

¹⁵ Cf., e.g., M. L. Goldberger and K. M. Watson, *Collision Theory* (John Wiley & Sons, New York, 1964), Secs. 6.8 and 11.4

where J_0 is the Bessel function of order zero, and $Q = k - p \simeq m^2/2k$ is the longitudinal momentum transfer.

Equation (14) can be integrated analytically at $\theta=0$ if the density distribution is uniform. It is natural to write $F = F_{\text{in}} + F_{\text{out}}$ where "in" and "out" refer to decay inside and outside the nucleus. Then

$$F_{\text{out}}(0, m) = 2\pi n \Delta(m) E(iu - iQ - \mu_a), \quad (15a)$$

$$F_{\text{in}}(0, m) = \frac{2\pi n}{ip} \frac{1}{iu + \mu_\pi - \mu_a} \times [E(iu - iQ - \mu_a) - E(-iQ - \mu_\pi)], \quad (15b)$$

where $1/u = p\Delta(m)$, and $\mu_a \equiv n\sigma_{\rho N}$, and $\mu_\pi \equiv 2n\sigma_{\pi N}$ are the inverse mean free paths for ρ absorption and 2π absorption in a nuclear medium of density n . Note also that when $m = m_\rho$, $-iu = m_\rho \Gamma_\rho / p$, which is the inverse mean free path for ρ decay. The function $E(x)$ is given by

$$E(x) = \frac{2}{iQ - x} \left[\left(\frac{R}{iQ} + \frac{1}{Q^2} \right) e^{iQR} + \left(\frac{1}{x^2} - \frac{R}{x} \right) e^{xR} - \frac{1}{x^2} - \frac{1}{Q^2} \right]. \quad (16)$$

The DT result is a limiting case of (16). When $\Gamma_\rho \rightarrow 0$, $F_{\text{in}}/F_{\text{out}}$ becomes of order Γ_ρ at the peak of the resonance, and F_{out} reduces to the DT amplitude [see Eq. (13) in DT] except for the obvious Breit-Wigner factor $\Delta(m)$.

Our Eq. (16) incorporates the skewing of the mass curve due to the variation of the minimum momentum transfer Q with $\pi\pi$ mass, as well as the collision-broadening effects arising from interior decay.¹⁶ In fact, the mass spectrum associated with the interior amplitude F_{in} is very much broader than that of free decay. As one would expect, $F_{\text{in}}/F_{\text{out}} \rightarrow 0$ as the photon energy (or p) tends to infinity.

III. VECTOR DOMINANCE

Does vector-meson dominance imply any $\pi\pi$ -mass dependence of the production amplitude beyond that explicitly shown in the preceding discussion? As we have seen, there are obvious m dependences arising from the longitudinal momentum transfer Q , the p -wave decay width $\Gamma_\rho(m)$, and the Green's function Y . There are other possible sources of m dependence not yet discussed: (i) in the vertex $\gamma_{\rho\pi\pi}$, (ii) in the vacuum propagator $\Delta(m)$, which can be expected to be a more complicated function of m than the naive Breit-Wigner form, and (iii) in the basic one-nucleon production amplitude $f_{\rho N}$. Indeed, it is the contention of Ross and Stodolsky¹⁰ that vector dominance requires $f_{\rho N}$ to vary as $(m_\rho/m)^2$ for m near m_ρ .

¹⁶ The qualitative features of Eq. (15) can also be understood from a naive statistical argument. See the Appendix.

We confine ourselves to a very brief recapitulation of the fundamental predictions of vector dominance.^{17,18} Let j_μ be the electromagnetic current, and let $|a\rangle$ and $|b\rangle$ be the arbitrary hadronic states with momenta p_a and p_b . The assumption that the photon and ρ^0 are both coupled to the hadronic isovector current implies that

$$\langle b | j_\mu | a \rangle = \frac{em_\rho^2}{2\gamma_\rho} \frac{1}{t - m_\rho^2 - \Pi(t)} M_\mu^{ba}(t). \quad (17)$$

Here γ_ρ is defined by the ρ -to-vacuum matrix element $\langle \rho | j_\mu | 0 \rangle = (m_\rho^2/2\gamma_\rho) \epsilon_\mu [(2\pi)^3 2m_\rho]^{-1/2}$, with ϵ_μ the ρ 's polarization vector; $t = (p_a - p_b)^2$; $\Pi(t)$ is the ρ 's vacuum polarization; and M_μ^{ba} is the proper vertex for $a + \rho^0 \rightarrow b$, i.e., the sum of all graphs that cannot be severed into two portions by cutting a single ρ line. By definition, $\Pi(m_\rho^2) = -im_\rho \Gamma_\rho(m_\rho)$. Furthermore, by construction, M_μ^{ba} does not contain any pole in the vicinity of $t \approx m_\rho^2$, and on the ρ mass shell it therefore can be identified as the amplitude that would describe the process $a + \rho^0 \rightarrow b$, with ρ^0 stable.

Under appropriate circumstances, $M_\mu^{ba}(t)$ can be measured near $t = m_\rho^2$. For example, in the reaction $\pi N \rightarrow \rho N$, this can be done fairly directly, while for the process $\rho N \rightarrow \rho N$ it must be done somewhat indirectly by an analysis of the type described in Sec. II. Relationships between ρ -induced hadronic and electromagnetic processes can then be obtained by assuming that the t dependence of $\langle b | j_\mu | a \rangle$ in the vicinity of the photoproduction point $t=0$ is determined predominantly by the ρ propagator in (17), i.e., by assuming that M_μ^{ba} at $t \approx 0$ does not differ appreciably from its measured value at $t \approx m_\rho^2$. In the present formulation one must also make the annoying additional assumption that $\Pi(0) \ll m_\rho^2$. For photoproduction, this assumption of ρ dominance thus yields

$$T(\gamma + a \rightarrow b) = (e/2\gamma_\rho) T(\rho^0 + a \rightarrow b), \quad (18)$$

where the T 's are the on-shell amplitudes for the indicated reactions, with the incoming ρ^0 treated as if it were stable. In particular, the amplitude $f_{\rho N}$ that appears in (1) is then given by¹⁹

$$f_{\rho N} = (ie/8\pi\gamma_\rho) p \sigma_{\rho N}. \quad (19)$$

When (19) is substituted into (1), the factors $-ipn(r)\sigma_{\rho N}$ combine to form the optical potential $U(r)$, and (1) becomes proportional to the amplitude for the strong process $\rho^0 + A \rightarrow A + 2\pi$. It is this proportionality which is the hallmark of vector dominance.

In the argument of Ross and Stodolsky, the direct

ρ -photon interaction is used instead of the assertion that the ρ and photon are coupled to the same current. But these two viewpoints only differ by a canonical transformation,²⁰ and are therefore physically equivalent. As we have just seen, vector dominance does not imply any rapid variation of $f_{\rho N}$ with $\pi\pi$ mass. Vector dominance is a *general* statement about the photon in the process $\gamma + a \rightarrow b$, valid for *arbitrary* states a and b , where b need not contain any pions whatsoever. Furthermore, the invariant mass of the photon line in the process $\gamma + a \rightarrow b$ is lightlike or spacelike, whereas the $\pi\pi$ mass m is always larger than $2m_\pi$. Should the Ross-Stodolsky hypothesis concerning the m dependence of $f_{\rho N}$ nevertheless turn out to be correct,²¹ it would have to be understood as a consequence of aspects of the production mechanism beyond those associated with the vector-meson-photon coupling.

The $\pi\pi$ -mass dependence of $\gamma_{\rho\pi\pi}$ and $\Delta(m)$ makes its appearance in the pion form factor, most particularly in the leptonic decay of the ρ . As we have already mentioned in Sec. II (cf. Ref. 14), there is no reason to believe that there is any unexpected rapid m variation of these functions in the vicinity of m_ρ .

IV. COMPARISON WITH DATA

As we have already pointed out, the precise mass dependence of $\Gamma_\rho(m)$ is a controversial subject which, fortunately, is not of great importance as long as one confines oneself to the mass region near the resonance. In the calculation reported here we have simply taken $\Gamma_\rho(m)$ as given by Eq. (4), with $\gamma_{\rho\pi\pi}$ having the constant value appropriate to a width at $m = m_\rho$ of 120 MeV as reported by the Cornell group⁶ and which is very close to the "best" value of 122 MeV determined by Roos and Pišut.²²

The nuclear density distribution $n(r)$ also enters into

²⁰ See Appendix B of Kroll, Lee, and Zumino, Ref. 18; K. Gottfried and D. R. Yennie, Phys. Rev. **182**, 1595 (1969).

²¹ Ross and Stodolsky (RS) (Ref. 10) give three arguments leading to the factor $(m_\rho/m)^2$. (I) In their Ref. 14, and in Sec. II B, they apparently assume the relationship $\langle b | j_\mu | a \rangle = (em_\rho^2/2\gamma_\rho) \times M_\mu^{ba}(t)$, to use our notation. As shown in Eq. (17), the denominator in this equation should read $m_\rho^2 + \Pi(t) - t$. (II) In Sec. II A, especially their Eq. (3), the eigenvalue in the Green's function must be the energy at which the collision takes place, which is the photon's incident energy k , and not $\omega(q)$. Thus their Eq. (3) should read $\psi_q^{(-)} = e^{iq \cdot x} [1/(H_0 - k - i\epsilon)] U \psi_q^{(-)}$. When this change is made, Eq. (4) of RS agrees with our Eqs. (5) and (18). (III) In Sec. V, RS employ the bilinear $\rho\gamma$ coupling, and assume that $\omega(k)$, the ρ^0 energy in nuclear matter, equals $(k^2 + m^2)^{1/2}$, where m is the *observed* $\pi\pi$ mass. We do not understand the justification for this assumption. Furthermore, their $\rho\gamma$ interaction is not gauge-invariant, because the A^2 term is deleted. As a consequence, the eigenvalue of their matrix H pertaining to the photon in vacuum does not have the form appropriate to a massless particle.

Stodolsky has shown [Phys. Rev. Letters **18**, 973 (1967)] that the m^{-2} factor does occur in the Drell diagram, wherein the photon dissociates into two pions, one of which is scattered diffractively by the nucleus. What remains unclear, however, is whether this diagram (when augmented with a final-state $\pi\pi$ interaction) alone accounts for the ρ -production amplitude, or whether it is merely a background contribution.

²² Matts Roos and Ján Pišut, Nucl. Phys. **B10**, 563 (1969).

¹⁷ M. Gell-Mann and F. Zachariasen, Phys. Rev. **124**, 953 (1961).

¹⁸ For recent reviews, see N. M. Kroll, T. D. Lee, and B. Zumino, Phys. Rev. **157**, 1376 (1967); N. M. Kroll, in *Proceedings of the Fourteenth International Conference on High-Energy Physics, Vienna, 1968* (CERN, Geneva, 1968), p. 75.

¹⁹ Here we assume that the forward ρN elastic amplitude is pure imaginary. For further discussion of this point see Sec. IV.

our calculations. We have assumed a diffuse distribution of the Woods-Saxon type²³

$$n(r) = \frac{n_0}{\{1 + \exp[(r-c)/a]\}},$$

with a half-density radius $c = (1.1A^{1/3} + 1) \times 10^{-13}$ cm and a skin thickness parameter $a = 2.40 \times 10^{-13}$ cm, independent of A . Effects on the production cross section of variation in the assumed density distribution are discussed below.

In the calculations presented here we have not attempted to fit the A dependence of the forward cross section by varying the cross section $\sigma_{\rho N}$ or the mass m_ρ ; a search for best values of these parameters entails important corrections for the finite angular aperture of the DESY spectrometer. To the extent that we understand them, these corrections have been included in our determination of the ρ -photon coupling constant from the data of Ref. 3 on Pb at 4.5 GeV/c. But we have not been able to evaluate the aperture corrections to the relative cross section data as a function of A as reported in Ref. 3. Consequently, we have simply adopted the value $\sigma_{\rho N} = 38$ mb as determined in Ref. 6, and taken $m_\rho = 765$ MeV. A total π - N cross section of 30 mb has been used throughout.

A. $\pi\pi$ -Mass Spectra at $\theta = 0^\circ$

In Figs. 1-5 we show $d\sigma/d\Omega dm$ at $\theta = 0^\circ$, normalized arbitrarily to unity at the resonance peak. The absolute magnitude of the cross section will be discussed below.

Figure 1 concerns Pb at $p = 4.5$ GeV/c. The solid curve is computed from our theoretical expression (14) with $\Gamma_\rho(m_\rho) = 120$ MeV; the dots show the result of the same calculation for $\Gamma_\rho(m_\rho) = 108$ MeV, which is the upper limit for the ρ width given by the Novosibirsk storage-ring experiment and very close to the value of 111 MeV for the width parameter at resonance obtained from the similar experiment by the Orsay group.¹¹ For comparison we show with a dashed curve the mass distribution arising from a Breit-Wigner form with $\Gamma_\rho(m_\rho) = 120$ MeV. The difference between the dashed and solid curves is due to the propagation of the unstable ρ through nuclear matter and the m dependence of the minimum momentum transfer Q . It is clear that the solid curve provides an excellent fit to the raw DESY data which is also shown. By raw we mean the experimental histogram without any nonresonant background subtraction. The fit at $\Gamma_\rho(m_\rho) = 108$ MeV is not satisfactory, however; this demonstrates that the effects due to the ρ 's instability cannot account for the

²³ For recent discussions of nuclear density determinations in the high-energy regime, see R. J. Glauber in *High Energy Physics and Nuclear Structure*, edited by G. Alexander (North-Holland Publishing Co., Amsterdam, 1967); B. Margolis, *Nucl. Phys. B4*, 433 (1968). Our value of nuclear skin thickness is the same as that found necessary by the above authors to explain various inelastic reactions. We have used half-density radii slightly larger than their choice of $c = 1.07A^{1/3} \times 10^{-13}$ cm.

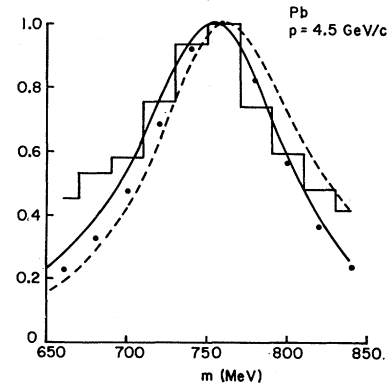


FIG. 1. $d\sigma/d\Omega dm$ in the forward direction as a function of $\pi\pi$ mass m . The target is Pb, the ρ momentum is 4.5 GeV/c, the ρ mass is 765 MeV, and the total ρN cross section is $\sigma_{\rho N} = 38$ mb. All curves, as well as the data, are normalized arbitrarily to unity at the peak. The solid curve is the theoretical mass distribution for a width Γ_ρ given by Eq. (4) with $\gamma_{\rho\pi\pi} = \text{const}$ and $\Gamma_\rho(m_\rho) = 120$ MeV, while the solid dots are for $\Gamma_\rho(m_\rho) = 108$ MeV. The dashed curve is an ordinary Breit-Wigner mass distribution for $\Gamma_\rho(m_\rho) = 120$ MeV. The experimental histogram is from Ref. 3.

difference between the ρ width as observed in nuclear photoproduction and in e^+e^- annihilation.

In Figs. 2 and 3 the theoretical curves are compared with the DESY data at $p = 4.5$ GeV/c for Cu and C. As always, $\sigma_{\rho N} = 38$ mb, and the mass-dependent width Γ_ρ is given by (4) with the value 120 MeV at $m = m_\rho$. The fit deteriorates with decreasing nuclear size, and is quite unsatisfactory for C. It must be emphasized, however, that we have made no background subtraction here, whereas the analysis of Ref. 3, which is based on the Ross-Stodolsky mass distribution, involves a significant (and arbitrary) background subtraction. In our opinion the most meaningful confrontation between theory and experiment occurs for the heaviest nuclei, where incoherent processes provide the smallest background. We therefore feel that the good fit displayed in Fig. 1 for Pb is really significant and very encouraging, while the disagreement found for C merely shows that physics is complicated under all but the most exceptional circumstances.

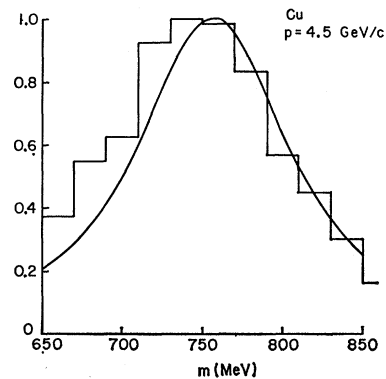


Fig. 2. Same as Fig. 1, but for Cu.

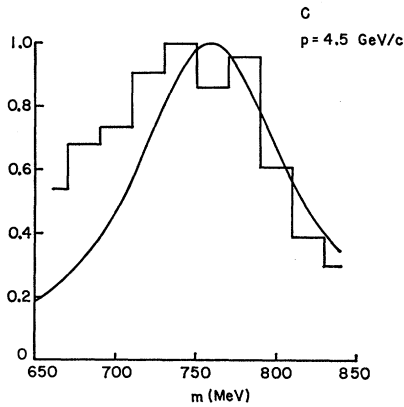


FIG. 3. Same as Fig. 1, but for C.

Figures 4 and 5 show the energy dependence of the corrections to the mass distributions arising from the ρ instability for Pb and C. As we see, these corrections are really quite large for Pb at the lowest DESY energy, $p=2.7$ GeV/c, and as expected, decrease rapidly as p increases.

Figure 6 shows the effect on the Pb $p=4.5$ GeV/c $\pi\pi$ -mass plot of nonzero real parts in the ρ -nucleon and π -nucleon forward elastic scattering amplitudes. The plotted quantity is $A^{-1}|f_{\rho N}|^{-2}d\sigma/d\Omega dm^2$, again computed from (14) with the trivial modifications $\sigma_{\pi N} \rightarrow \sigma_{\pi N}(1-i\alpha_{\pi N})$ and $\sigma_{\rho N} \rightarrow \sigma_{\rho N}(1-i\alpha_{\rho N})$ in the optical potentials for the π and ρ , and hence in Eqs. (11) and (13).²⁴ Here $\alpha_{\pi N}$ and $\alpha_{\rho N}$ are the ratios of real to imaginary part of the π -N and ρ -N forward-scattering amplitudes. As expected, the result is only very weakly dependent on $\alpha_{\pi N}$, since at the energy in question the ρ almost always escapes the region of non-negligible target

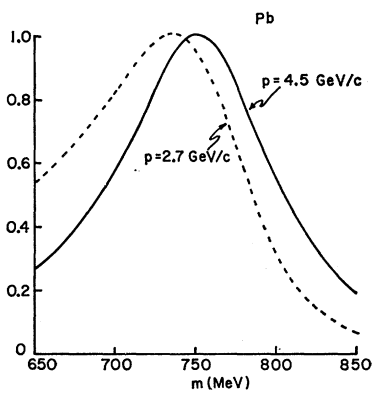


FIG. 4. Energy dependence of $\pi\pi$ mass distribution for Pb. The differential cross section $d\sigma/d\Omega dm^2$ in the forward direction normalized to unity at the peak is shown for $p=2.7$ and 4.5 GeV/c. $\Gamma_{\rho}(m_{\rho})=120$ MeV.

²⁴ The corrections to the total cross sections $\sigma_{\pi N}$ and $\sigma_{\rho N}$ in (11) and (13) do, in fact, have the same and not the opposite sign, since the pion wave functions in (5) satisfy incoming spherical wave boundary conditions which call for the time-reversed (i.e., complex-conjugated) form of the usual optical potential.

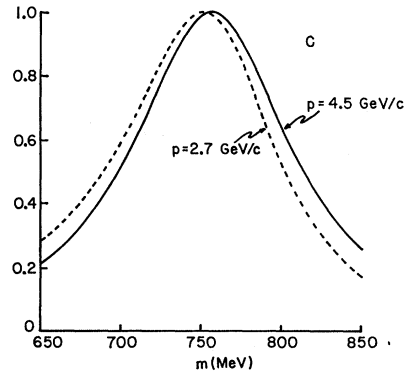


FIG. 5. Same as Fig. 4, but for C.

density prior to decay, even in a Pb target. We see, however, that the mass plot is sensitive to a refractive component in the optical potential seen by the ρ . Furthermore, the correction to the forward nuclear cross section for nonzero values of $\alpha_{\rho N}$ is of the same sign as $\alpha_{\rho N}$. This can be easily understood from the much simpler DT model with a uniform nuclear density distribution. In this approximation the contribution to the nuclear production amplitude from each impact parameter b is $f(b, Q)$, where

$$f(b, Q) = \int_{z \leq R^2 - b^2} dz e^{iQz} \exp(n_0 \sigma_{\rho N} z / 2),$$

where n_0 is the central nuclear density and Q is the minimum momentum transfer $k-p$. The dependence of the forward production amplitude on the sign of $\alpha_{\rho N}$ is then clear from the fact that $f(b, Q)$ is a decreasing function of Q , while the contribution of each impact parameter to the amplitude for nonzero $\alpha_{\rho N}$ is $f(b, Q - \frac{1}{2}n_0\sigma_{\rho N}\alpha_{\rho N})$.

The reader may have noticed that we have only shown mass distributions over the interval $650 < m < 850$

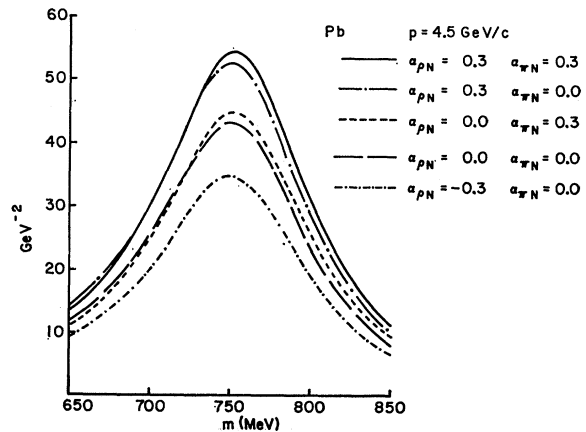


FIG. 6. Dependence of the $\pi\pi$ mass distribution for Pb on the real parts of the ρN and πN scattering amplitudes. The plotted cross section is $A^{-1}|f_{\rho N}|^{-2}(d\sigma/d\Omega dm^2)$ in the forward direction.

MeV. Recently, the wings of the ρ resonance have attracted a good deal of attention,^{4,14} and it is our intention to counteract this tendency. It is well known in various branches of physics that one can only discuss the wings of a resonance if one has a detailed dynamical understanding of the mechanism responsible for the resonance. Such an understanding is certainly lacking in the case of the ρ , and for safety's sake it is best to confine one's attention to a region no larger than $(m_\rho - \Gamma_\rho) < m < (m_\rho + \Gamma_\rho)$.

B. Angular Distributions

The angular distribution of coherent ρ production is shown in Figs. 7-15. These are plotted as functions of the production angle θ in milliradians instead of the more fashionable momentum transfer variable t , because the latter is a function of the $\pi\pi$ mass m . It should also be said that there is not too much merit in fitting the differential cross sections to exponentials in t , because the density distribution of heavy nuclei is far from Gaussian. We find that on the whole the extension of the DT formula to finite angles agrees exceedingly well with the angular distribution evaluated from our Eq. (14). In Fig. 7 we show angular distributions at $p=4.5$ GeV/c for a variety of nuclei. In this and succeeding figures, unless specified otherwise, the plotted quantity is $A^{-1}|f_{\rho N}|^{-2}d\sigma/d\Omega$, where the mass integration extends over the interval $650 < m < 850$ MeV with both π and ρ optical potentials purely absorptive. In Fig. 7 the difference between our Eq. (14) evaluated at $m=m_\rho$

and the DT formula [modified by the Breit-Wigner factor $\Delta(m_\rho)$] would barely be perceptible to the unaided eye.

At lower energy and for heavy nuclei the angular distributions have a more curious and interesting behavior. In Fig. 8 we show the predictions of Eq. (14) for Pb as a function of energy. The plotted quantity is the same as in the previous figure but normalized to unity in the forward direction at each energy. As we see, the secondary diffraction maximum grows with decreasing energy, and by $p=2.5$ GeV/c, the first diffraction minimum has disappeared entirely. In this region the angular distribution also depends quite sensitively on m , as shown in Figs. 9 and 10 for Cu and Pb at $p=2.7$ GeV/c. The ordinate in these figures is $A^{-1}|f_{\rho N}|^{-2}d\sigma/d\Omega dm^2$.

Figures 11 and 12 show the dependence of the angular distribution on the parameters of the ρ -nucleon interaction. In Fig. 11 we show the effect on the Pb $p=4.5$ GeV/c cross section of a possible real part in the ρ - N forward amplitude. The π - N forward amplitude, to which the results are highly insensitive, has been kept pure imaginary. We see that the diffraction minimum becomes increasingly filled in as $\sigma_{\rho N}$ progresses from negative to positive values. Figure 12 indicates the dependence of the nuclear cross section on $\sigma_{\rho N}$, again for a Pb target at $p=4.5$ GeV/c. As $\sigma_{\rho N}$ is increased, the cross section is reduced at all angles due to the increased absorption, except in the region of the diffraction minimum, which is slightly filled in. It should be borne in mind, however, that the cross sections of Fig. 12

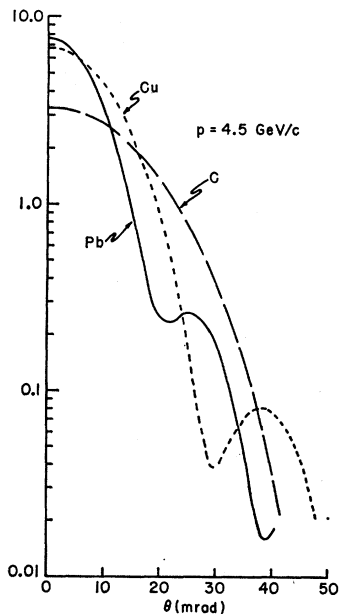


FIG. 7. $A^{-1}|f_{\rho N}|^{-2}(d\sigma/d\Omega dm^2)$ integrated over $650 < m < 850$ MeV at $p=4.5$ GeV/c for C, Cu, and Pb. At this energy, our Eq. (14) evaluated at $m=m_\rho$ yields angular distributions which are in excellent agreement with those calculated with the Drell-Trefil formula.

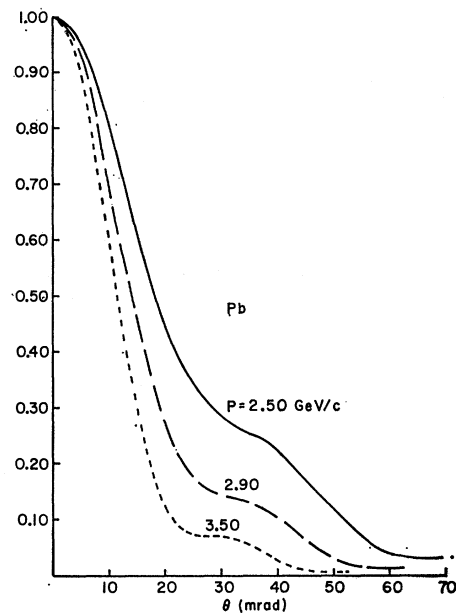


FIG. 8. Dependence of angular distribution on ρ momentum for Pb. The ordinate is the same quantity as plotted in the previous figure, normalized to unity at $\theta=0$. Corresponding curves calculated with the DT formula agree with our result evaluated at $m=m_\rho$.

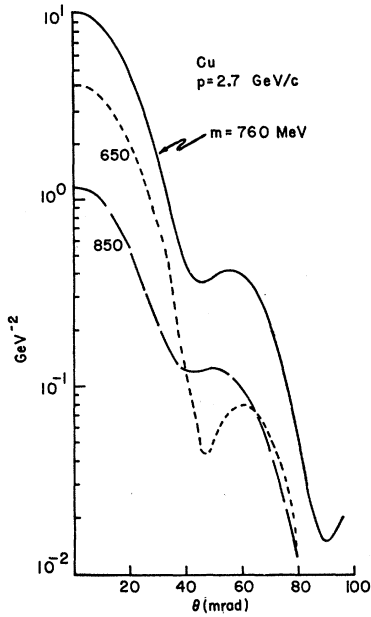


FIG. 9. Dependence of $A^{-1}|f_{\rho N}|^{-2}(d\sigma/d\Omega dm^2)$ on $\pi\pi$ mass m for Cu at $p=2.7$ GeV/c.

have had a factor $|f_{\rho N}|^2$ divided out. If this factor is included via the vector-dominance prescription $f_{\rho N} \propto \sigma_{\rho N}$, the extra factor of $\sigma_{\rho N}^2$ will cause the cross section to *increase* with increasing $\sigma_{\rho N}$ at all angles. The relative increase is found to be greatest in the region of the diffraction minimum, so that the minimum still appears to fill in with increasing $\sigma_{\rho N}$.

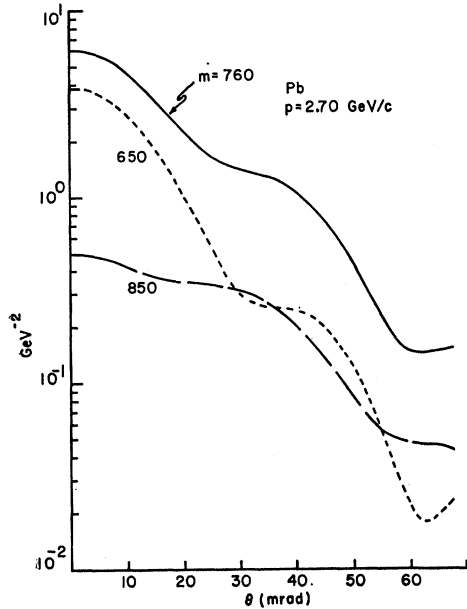


FIG. 10. Same as Fig. 9, but for Pb.

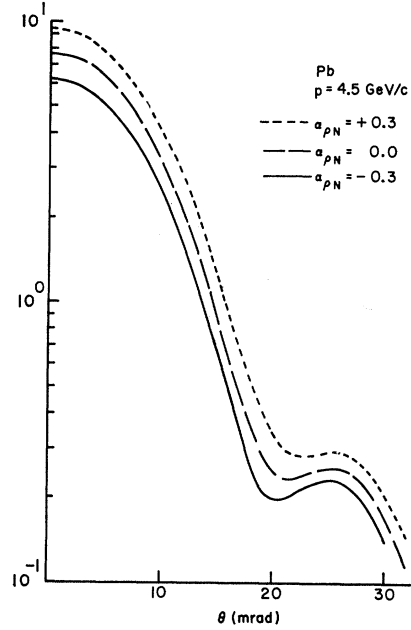


FIG. 11. Dependence of angular distribution on the real part of the ρN scattering amplitude for Pb at $p=4.5$ GeV/c. The ordinate is the same quantity as in Fig. 7.

C. Sensitivity to Nuclear Properties

Finally, we turn our attention to the dependence of the predictions of (14) on target parameters. Specifically the two effects we consider are (i) variation in the form of the independent particle density function chosen, and (ii) modification of the optical potentials due to

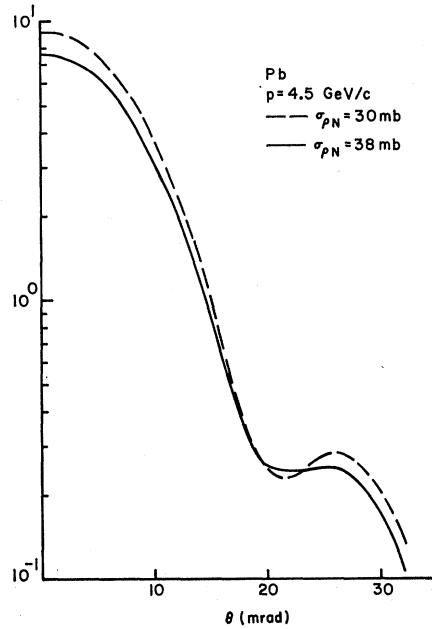


FIG. 12. Dependence of angular distribution on $\sigma_{\rho N}$ for Pb at $p=4.5$ GeV/c. The ordinate is the same quantity as in Fig. 7.

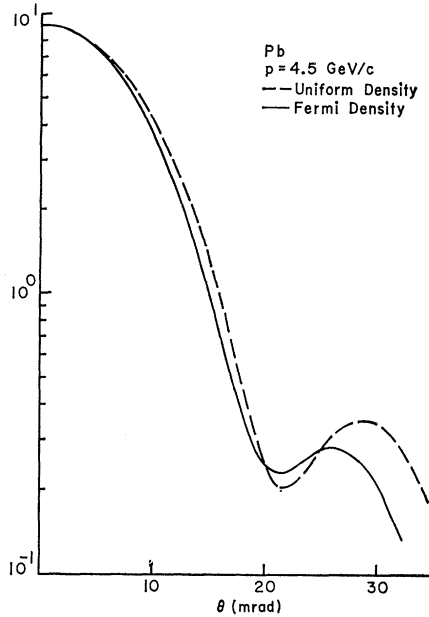


FIG. 13. Dependence of angular distribution on nuclear shape for Pb at 4.5 GeV/c. The plotted quantity is the same as in Fig. 7, but with $\sigma_{\rho N}=30$ mb, $\Gamma_{\rho}(m_{\rho})=125$ MeV.

correlations among target nucleons. As far as (i) is concerned, the cross section is expected to be rather insensitive to the details of the nuclear density when the production angle θ vanishes. At angles near and beyond the first diffraction minimum one would, however, expect some sensitivity to the nuclear shape. The same may in fact be true at $\theta=0$ if the minimum momentum transfer Q becomes comparable to the reciprocal of the rms nuclear radius, i.e., in the heaviest nuclei and at sufficiently low energy. Figures 13 and 14 compare, for a Pb target and $p=4.5$ and 2.7 GeV/c, respectively, the angular distributions for the Woods-Saxon distribution described earlier and for a uniform spherical nucleus. In these curves, $\Gamma_{\rho}(m_{\rho})=125$ MeV and $\sigma_{\rho N}=30$ mb.

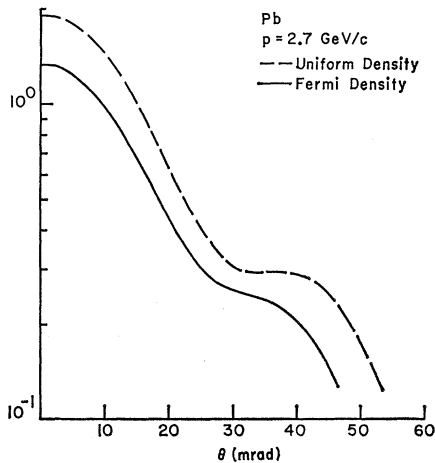


FIG. 14. Same as Fig. 13, but at $p=2.7$ GeV/c.

As expected at 4.5 GeV/c, the results for the two distributions are indistinguishable at $\theta=0$, while for the smoother Woods-Saxon shape, the secondary maximum is suppressed. At the lower energy the sensitivity to the nuclear edge is considerably greater; the angular distribution is lowered in magnitude at all angles for the Woods-Saxon shape, with a suppression of about 30% even for forward production. This large an effect could, in fact, be anticipated from the sensitivity to nuclear shape of the body form factor alone. The ratio of Woods-Saxon to uniform-density form factors is, to second order in the skin thickness and all orders in the momentum transfer q ,

$$1 - (\pi a/c)^2 [1 - \frac{1}{6}x^2 - \frac{1}{3}x^3(\tan x - x)^{-1}],$$

where $x=qc$; a and c are the parameters of the Woods-Saxon distribution defined earlier.²⁵ For a value of q corresponding to the minimum momentum transfer Q , this ratio assumes the values 0.92 and 0.68 for the parameter values of Figs. 13 and 14, respectively.

The effects of pairwise correlations among the target nucleons can be incorporated into the theory by replacing the optical potentials $U_i(r) = -ip_i\sigma_{iN}n(r)$ by the quantities²⁶

$$U_i'(r) = U_i(r) [1 - \frac{1}{2}n(r)\sigma_{iN}R_c].$$

Here, i stands for either ρ or π , and R_c is the correlation length defined by

$$R_c = \int_0^{\infty} dx G(x),$$

where the pair correlation function $G(x)$ is given by

$$p^{(2)}(\mathbf{x}, \mathbf{x}') = p^{(1)}(\mathbf{x})p^{(1)}(\mathbf{x}') [1 + G(\mathbf{x}, \mathbf{x}')].$$

Here $p^{(2)}(\mathbf{x}, \mathbf{x}')$ is the probability of two nucleons occupying positions \mathbf{x}, \mathbf{x}' , and $p^{(1)}(\mathbf{x}) = A^{-1}n(\mathbf{x})$. For a very extensive system such as the Pb nucleus, we make only a small error (near the nuclear surface) by assuming a translationally invariant form $G(\mathbf{x}, \mathbf{x}') = G(|\mathbf{x} - \mathbf{x}'|)$ as indicated in the definition of R_c . One crude estimate of R_c is provided by the degenerate Fermi-gas model for the ground state of the target nucleus²⁶; in this case,

$$R_c = -3\pi/20p_F, \quad (20)$$

where p_F is the Fermi momentum. The resulting correction to the potential when $\sigma_{\rho N}=30$ mb is about 6%.

In an ideal Fermi gas the correlations simulate the effect of a purely repulsive force, as is shown by the negative sign of (20). The repulsive core of the nuclear force will decrease R_c even further, but the attractive portion of the force field will have the opposite effect. It is not possible to estimate the net result of these

²⁵ For evaluation of integrals of the Fermi type see, e.g., L. D. Landau and E. M. Lifshitz, *Statistical Physics* (Addison-Wesley Publishing, Co., Inc., Reading, Mass., 1958), Article 57.

²⁶ See, e.g., Ref. 15, Sec. 11.4. We simplify the problem by treating nuclear protons and neutrons as indistinguishable.

various tendencies without a detailed calculation of $G(x)$. Such a calculation falls outside the scope of this paper, and we have confined ourselves to showing the predictions of the theory for Pb at 4.5 GeV/c in Fig. 15 for $R_c = -0.4 \times 10^{-13}$ cm, corresponding to purely statistical Fermi correlations, and also for $R_c = -0.8 \times 10^{-13}$ cm. The actual value of R_c should certainly lie between zero and -0.8×10^{-13} cm.

We see that the correlation effects are negligible at large production angles, and increase to a maximum at $\theta = 0$. It should be noted that the correlation effects are sensitive to the shape of the one-particle density distribution; for a uniform nuclear shape, the correction to the optical potentials for $R_c < 0$ are effectively no more than increases in the central density, of which the forward cross section is an increasing, not a decreasing function.

Two remarks concerning these angular distributions are in order: (i) The low-energy behavior of the angular distribution discussed in connection with Fig. 8 appears to explain why the DESY data on Pb [see Fig. 2(c) in Ref. 3] fails to show any vestige of a diffraction minimum near the zero of the function $J_1(\rho c \theta)$; (ii) the rapid variation of the angular distribution with $\pi\pi$ mass, nuclear radius, and ρ momentum revealed in Figs. 8–10, and the dependence of the diffraction minimum depth on $\alpha_{\rho N}$ itself shown in Fig. 11, offer some hope that one may be able to determine the real part of the ρN scattering amplitude by careful measurements. It is of course necessary in any such determination to first extract from the experimental angular distribution the contribution of incoherent events, which completely

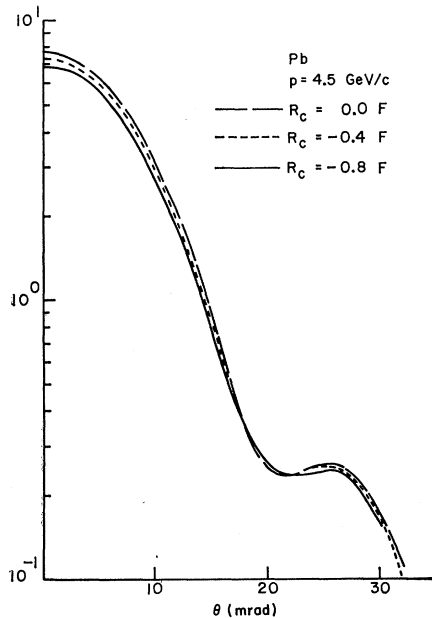


FIG. 15. Dependence of angular distribution on target nucleon correlations for Pb at 4.5 GeV/c. The ordinate and parameter values are as in Fig. 7.

fill in the diffraction minimum in all but the heaviest nuclei.²⁷

D. A Dependence of Forward Cross Section

We now turn to the A dependence of the forward cross section. In Tables I and II we list values of the forward cross section divided by $|f_{\rho N}|^2$ at the ρ peak, and also integrated over the interval $720 < m < 820$ MeV. The integrated quantity, as evaluated from the DT formula, is also given.²⁸ For simplicity, a uniform nuclear density of radius $R = 1.30A^{1/3} \times 10^{-13}$ cm has been used in these computations, with $\sigma_{\rho N} = 30$ mb and Γ_ρ assuming the m -independent value 125 MeV.²⁹ As anticipated in our introductory discussion (see also the Appendix), the correction to the magnitude of the DT cross section due to ρ instability is small—less than 15% at $p = 2.7$ GeV/c. Table I has one unexpected feature, however. For light nuclei, and at low energy (2.7 GeV/c), our cross section falls below that of DT, as expected, but for Pb our cross section is *larger* than that when the ρ 's instability is neglected. This surprising behavior³⁰ disappears at higher energy (see Table II).

TABLE I. (a) $A^{-1} f_{\rho N}^{-2} (d\sigma/d\Omega)$, integrated over $720 < m < 820$ MeV, including corrections due to ρ instability. (b) Same as (a), but using DT theory. (c) $A^{-1} f_{\rho N}^{-2} (df/d\Omega dm^2)$, at $m = m_\rho$, in units of GeV^{-2} . ($p = 2.7$ GeV/c.)

	(a)	(b)	(c)
Be	1.27	1.38	9.92
C	1.45	1.59	11.4
Al	1.84	2.08	14.5
Cu	1.78	2.01	14.0
Ag	1.47	1.58	11.5
Pb	0.97	0.91	7.51

TABLE II. (a), (b), and (c) are the same as in Table I. ($p = 4.5$ GeV/c.)

	(a)	(b)	(c)
Be	1.72	1.79	13.4
C	2.10	2.19	16.3
Al	3.39	3.62	26.5
Cu	4.92	5.35	38.5
Ag	5.64	6.18	44.3
Pb	6.00	6.55	47.3

²⁷ K. S. Kolbig and B. Margolis, Nucl. Phys. **B6**, 85 (1968).

²⁸ A direct comparison of the theoretical values in Tables I and II should not be made with the data in Fig. 1 of Ref. 3 because the latter already includes a very significant correction for the angular aperture of the DESY spectrometer.

²⁹ Computations for Tables I and II (which compare theoretical predictions only) were done prior to the appearance of the Cornell data (Ref. 6) and used the 30-mb value of Ref. 3 for $\sigma_{\rho N}$. For clarification, we remark that $\sigma_{\rho N} = 30$ mb and a mass-independent ρ width of 125 MeV have been used only for Tables I and II, the numerical results in the Appendix, and Figs. 13 and 14. All other results (in particular, all comparisons with experimental data) use $\sigma_{\rho N} = 38$ mb and $\Gamma_\rho(m)$ given by Eq. (4) with $\Gamma_\rho(m_\rho) = 120$ MeV.

³⁰ That this peculiar behavior is not due to a computational error has been carefully checked by a hand calculation of ρ production from a slab of nuclear matter.

E. Vector Dominance and γ_ρ

The problem of extracting γ_ρ from the data on ρ photoproduction has been carefully considered by the Cornell group⁶; we have nothing essential to add to their discussion. The instability corrections are certainly negligible at the high photon energies used at Cornell⁶ and SLAC.⁷ We therefore confine ourselves to the lower-energy DESY data. Even here the instability, and other corrections, discussed above have only a small effect on the vector-meson coupling constant as determined from the DESY data.⁴ In our determination of γ_ρ , we compare with the results of Ref. 3 the cross section predicted by (14) averaged over the reported angular aperture of 0.5° with the Woods-Saxon density distribution described previously, and $\Gamma_\rho(m)$ given by (4) normalized to 120 MeV at the ρ peak. In view of the difficulty described above regarding the determination of $\sigma_{\rho N}$ from the A dependence of the forward cross section as given in Ref. 3, we again take $\sigma_{\rho N} = 38 \pm 3$ mb as determined in Ref. 6. Finally, the computed coupling constants are for purely absorptive potentials with $R_c = -0.4 \times 10^{-13}$ cm corresponding to the inclusion of statistical correlations in the target. Values of $\gamma_\rho^2/4\pi$ increase by about 6% if R_c is set equal to zero. Results from the $p = 4.5$ GeV/ c data are then³¹

	$\gamma_\rho^2/4\pi$
C	0.37 ± 0.06
Cu	0.31 ± 0.06
Pb	0.35 ± 0.06

We should point out that in carrying out these calculations, we have not extrapolated the differential cross section to the unphysical point $t=0$.

It is quite clear that the instability corrections discussed in this article cannot begin to account for the discrepancy between the DESY data on the one hand, and those of SLAC and Cornell on the other.

Note added in proof. 1. A completely new series of measurements on ρ^0 photoproduction has recently been reported by the DESY group: H. Alvensleben *et al.*, Phys. Rev. Letters **23**, 1058 (1969). It now appears that $d\sigma/d\Omega dm^2$ as measured in this experiment is in very good agreement with Ref. 6, but that there is a discrepancy in the width ($\Gamma_{\text{DESY}} = 140 \pm 10$ MeV, $\Gamma_{\text{Cornell}} \approx 120$ MeV). As a consequence the values of $\sigma_{\rho N}$ that emerge from the two experiments *must* agree within the errors if the analysis is based on precisely the same theoretical assumptions. On the other hand, there should be a disagreement in $\gamma_\rho^2/4\pi$ of the order of the discrepancy in the widths. In comparing the results of the new DESY experiment with those of Ref. 6, one should note that Alvensleben *et al.* have included correlation corrections, and have also assumed that $\alpha_{\rho N} = -0.2$ in arriving at their final result. 2. A

³¹ For a fairly recent survey of ρ coupling constants, see Ref. 7, and also S. C. C. Ting and N. M. Kroll, Refs. 11 and 18.

considerably more refined evaluation of the correlation correction can be found in G. von Bochman *et al.*, Phys. Letters **30B**, 254 (1969).

ACKNOWLEDGMENTS

We should like to thank D. R. Yennie for numerous remarks and criticisms. We have also benefited from informative discussions with W. K. Bertram, L. N. Hand, D. Leith, A. Silverman, and S. C. C. Ting.

APPENDIX

An intuitive argument concerning the effects of the ρ 's instability may help to clarify qualitative aspects of the results of our detailed calculations. For this purpose we define three mean free paths: $1/\mu_a \equiv 1/n\sigma_{\rho N}$ for nuclear absorption of a ρ , $1/\mu_\pi \equiv 1/2n\sigma_{\pi N}$ for nuclear absorption of two pions, and $1/\mu_d \equiv p/m_\rho\Gamma_\rho$ for natural decay of a ρ . Associated with each of these, there is a probability for disappearance in a distance x , e.g., $P_a(x) = e^{-\mu_a x}$, etc.

Our aim is to estimate the importance of ρ decay inside the nucleus by a simple statistical argument. Consider photoproduction in a slab of thickness $D = \frac{4}{3}R$, which is the mean thickness of a sphere of radius R . Let $(N_0/D)dz$ be the number of ρ 's photoproduced in a slab of thickness dz . Ignoring decay, the total number of photoproduced ρ 's is

$$N_{\text{DT}} = \frac{N_0}{D} \int_0^D dz P_a(D-z). \quad (\text{A1})$$

Within the context of these simple considerations, (A1) is the analog of the DT calculation.

When decay is taken into account, it is natural to separate N , the total number of ρ events, into two parts, $N = N_{\text{out}} + N_{\text{in}}$. Here N_{out} is the total number of ρ 's that decayed outside the nucleus:

$$\begin{aligned} N_{\text{out}} &= \frac{N_0}{D} \int_0^D P_a(D-z) P_d(D-z) dz \\ &= \frac{N_0}{D} \frac{1}{\mu_a + \mu_d} [1 - P_a(D) P_d(D)]. \end{aligned} \quad (\text{A2})$$

N_{in} is the number of ρ events that arise from interior decay. The number of ρ 's of energy E decaying in a slab of thickness dz' at z' is the product of the decay rate $m_\rho\Gamma_\rho/E$, the time spent in this slab $(p/E)^{-1}dz'$, and the number of ρ 's arriving at z' , which is

$$\frac{N_0}{D} \int_0^{z'} P_a(z'-z) P_d(z'-z) dz.$$

The probability that the decay pions escape is

$P_\pi(D-z')$, whence

$$N_{\text{in}} = \frac{N_0}{D} \mu_d \int_0^D dz' P_\pi(D-z') \int_0^{z'} dz P_a(z'-z) P_d(z'-z) \\ = \frac{\mu_d}{\mu_\pi - \mu_d - \mu_a} \left(N_{\text{out}} - \frac{N_0}{D} \frac{1}{\mu_\pi} [1 - P_\pi(D)] \right). \quad (\text{A3})$$

One can verify that the quantum-mechanical *amplitudes* F_{in} and F_{out} of Eq. (15), evaluated on the ρ peak ($m=m_\rho$), have essentially the same form as the *probabilities* N_{in} and N_{out} .

Some results obtained with these equations are listed as follows for $p=2.7$ GeV/ c (we have used $\sigma_{\rho N}=30$ mb, $\Gamma_\rho=125$ MeV, and $R=1.30A^{1/3}$ F):

	N/N_{DT}	$N_{\text{in}}/N_{\text{out}}$
C	0.93	0.21
Cu	0.87	0.25
Pb	0.85	0.27

We note that the discrepancy between the analog to the DT result, Eq. (A1), and $N_{\text{in}}+N_{\text{out}}=N$, is remarkably small even at this very low energy, and, what is perhaps more surprising, very slowly varying with A . The most important reason for the small departure of N/N_{DT} from unity is that the absorption mean free path $1/\mu_a$ is small compared to R . Hence in medium weight and heavy nuclei, photoproduced ρ 's predominantly originate from the "downstream end" of the nucleus, where the ρ has relatively little difficulty in escaping before decay. Furthermore, some of the decay pions from interior decay also manage to escape, and are counted as ρ events.

The statistical argument does not provide a mass distribution for interior decays. Above all, it does not take the quantum-mechanical coherence of interior and exterior decay into account. Nevertheless, it serves as a useful supplement to the correct calculation described in the text.

Nature of $SU(3) \times SU(3)$ Symmetry Breaking—Results from a Systematic Test of the Soft-Meson Theorems*

FRANK VON HIPPEL†

Department of Physics, Institute of Theoretical Physics, Stanford University, Stanford, California 94305

AND

JAE KWAN KIM

Department of Physics, Harvard University, Cambridge, Massachusetts 02138

(Received 2 October 1969)

We make a systematic test of soft-meson-theorem predictions for both elastic and inelastic pseudoscalar-meson-baryon threshold scattering amplitudes. The predictions are obtained by using an extrapolation procedure developed by Fubini and Furlan and by ourselves. Our results give considerable support to a theory of $SU(3) \times SU(3)$ symmetry breaking proposed recently by Gell-Mann, Oakes, and Renner, and imply that, in the absence of symmetry breaking, the mass of the $J^P = \frac{1}{2}^+$ baryon octet would be approximately that of the physical nucleon.

I. INTRODUCTION

IN this paper we use the experimental values of the real parts of 13 elastic and inelastic pseudoscalar-meson-baryon (P - B) scattering amplitudes,

$$P_\alpha + B_i \rightarrow P_\beta + B_f, \quad (1.1)$$

evaluated at threshold, to test soft-meson theorems. A

brief report of some of our preliminary results has already been presented elsewhere.¹

The primary interest in the soft-meson theorems is that, at the moment, they afford us the best opportunity for testing experimentally forms which have been proposed for equal-time commutators of axial-vector charges with each other and with their time derivatives. Thus they allow us to test both the $SU(3) \times SU(3)$ charge-algebra hypothesis and the hypotheses concerning the nature of $SU(3) \times SU(3)$ symmetry breaking.

The difficulty in making these tests originates in the fact that the soft-meson theorems fix the values of the

* Research sponsored by the Air Force Office of Scientific Research, Office of Aerospace Research, U. S. Air Force, under AFOSR Contract No. F44620-68-C-0075 and the U. S. Atomic Energy Commission under Contract No. AEC AT(30-1)-2752.

† Alfred P. Sloan Foundation Fellow. Address 1969-70: Theory Group, Lawrence Radiation Laboratory, University of California, Berkeley, Calif.

¹ F. von Hippel and J. K. Kim, Phys. Rev. Letters **22**, 740 (1969).